ORIGINAL ARTICLE

Meta-QTL analysis of tan spot resistance in wheat

Yuan Liu[1] · Evan Salsman[1] · Runhao Wang[1] · Nelomie Galagedara[2] · Qijun Zhang[1] · Jason D. Fiedler[3] · Zhaohui Liu[2] · Steven Xu[4] · Justin D. Faris[4] · Xuehui Li[1] 🔵

Abstract

Key message **A total of 19 meta-QTL conferring resistance to tan spot were identified from 104 initial QTL detected in 15 previous QTL mapping studies.**

Abstract Tan spot, caused by the fungal pathogen *Pyrenophora tritici-repentis* (*Ptr*), is a major foliar disease worldwide in both bread wheat and durum wheat and can reduce grain yield due to reduction in photosynthetic area of leaves. Developing and growing resistant cultivars is a cost-effective and environmentally friendly approach to mitigate negative effects of the disease. Understanding the genetic basis of tan spot resistance can enhance the development of resistant cultivars. With that goal, over 100 QTL associated with resistance to tan spot induced by a variety of *Ptr* races and isolates have been identified from previous QTL mapping studies. Meta-QTL analysis can identify redundant QTL among various studies and reveal major QTL for targeting in marker-assisted selection applications. In this study, we performed a meta-QTL analysis of tan spot resistance using the reported QTL from 15 previous QTL mapping studies. An integrated linkage map with a total length of 4080.5 cM containing 47,309 markers was assembled from 21 individual linkage maps and three previously published consensus maps. Nineteen meta-QTL were clustered from 104 initial QTL projected on the integrated map. Three of the 19 meta-QTL located on chromosomes 2A, 3B, and 5A show large genetic effects and confer resistance to multiple races in multiple bread wheat and durum wheat mapping populations. The integration of those race-nonspecific QTL is a promising strategy to provide high and stable resistance to tan spot in wheat.

✉ Xuehui Li
   Xuehui.li@ndsu.edu

1 Department of Plant Science, North Dakota State University, Fargo, ND 58108, USA

2 Department of Plant Pathology, North Dakota State University, Fargo 58108, USA

3 Biosciences Research Laboratory, USDA-ARS Genotyping Laboratory, Fargo, ND 58102, USA

4 USDA-ARS Cereal Crops Research Unit, Northern Crop Science Laboratory, Edward T. Schafer Agricultural Research Center, Fargo, ND 58102, USA

Introduction

Tan spot, also known as yellow spot, is a major foliar disease worldwide on both hexaploid bread wheat (*Triticum aestivum* L., $2n = 6x = 42$, AABBDD) and tetraploid durum wheat (*T. turgidum* L. $2n = 4x = 28$, AABB). Tan spot is caused by a fungal pathogen *Pyrenophora tritici-repentis* (*Ptr*) (Died.) anamorph *Drechslera tritici-repentis* (Died.) Shoemaker (synonym *Helminthosporium tritici-repentis*) and characterized by large lesions with tan-color surrounded by chlorotic haloes on the leaves of susceptible infected wheat lines. Tan spot can cause grain yield losses ranging from 5 to 31% due to a reduction in photosynthetic area of leaves (Shabeer and Bockus 1988; Bhathal et al. 2003). In Australia, annual loss due to tan spot was AUD212 M and potential loss could reach AUD676 M (Murray and Brennan 2009). Crop rotation and fungicide applications are viable practices to reduce the effect of tan spot. However, developing and growing resistant cultivars is more cost-effective and environmentally friendly. Understanding the genetic basis of

tan spot resistance can enhance the development of resistant cultivars.

Ptr produces necrotrophic effectors (NEs), also known as host-selective toxins (HSTs), which subvert the wheat immune system (Faris et al. 2013) and lead to necrotic and/or chlorotic lesions. Three *Ptr* NEs including Ptr ToxA, Ptr ToxB, and Ptr ToxC have been characterized. Ptr ToxA is a small protein and induces necrosis (Manning 2005). Ptr ToxB is also a protein but induces chlorosis rather than necrosis (Ciuffetti et al. 2010). Ptr ToxC is an unknown low weight molecule, and like Ptr ToxB, it also induces chlorosis but not necrosis (Effertz et al. 2002). Existence of a putative Ptr ToxD also was reported (Meinhardt et al. 2003; Ciuffetti et al. 2003). Some isolates do not produce Ptr ToxA but can induce necrosis, implicating the existence of other uncharacterized NEs (Ali et al. 2010; Guo et al. 2018). Currently, *Ptr* isolates are classified into eight races based on the three known NEs (Strelkov and Lamari 2003). Race 1 produces Ptr ToxA and Ptr ToxC; Race 2 produces Ptr ToxA; Race 3 produces Ptr ToxC; Race 4 produces none; Race 5 produces Ptr ToxB; Race 6 produces Ptr ToxB and Ptr ToxC; Race 7 produces Ptr ToxA and Ptr ToxB; and Race 8 produces all three known NEs.

Previous studies revealed that the interaction between wheat and the three known NEs follows an inverse gene-for-gene model (Ciuffetti et al. 2010), i.e., the recognition of a NE by a dominant host gene leads to susceptibility. Three dominant host sensitivity genes have been identified in wheat by evaluating reaction to infiltration of cultures containing NEs and named as *Tsn1*, *Tsc1*, and *Tsc2* (Singh et al. 2010; Faris et al. 2013). *Tsn1*, conferring sensitivity to Ptr ToxA, is located on chromosome 5B and was the first dominant sensitive gene cloned in wheat (Faris et al. 2010). *Tsn1* harbors serine/threonine protein kinase (S/TPK), nucleotide binding (NB), and leucine-rich repeat (LRR) domains. *Tsc1* is located on chromosome 1A and confers sensitivity to Ptr ToxC (Effertz et al. 2002). *Tsc2* located on chromosome 2B confers sensitivity to Ptr ToxB (Abeysekara et al. 2010; Friesen and Faris 2004; Orolaza et al. 1995). Dominant susceptibility loci were also found on chromosome 3A, 3B, and 3D (Singh et al. 2006, 2008; Tadesse et al. 2006, 2008), which might interact with other uncharacterized NEs. Cloning other dominant sensitivity genes will facilitate the understanding of the interactions between wheat and *Ptr* NEs.

In addition to the dominant host sensitivity genes, over 100 QTL associated with resistance to tan spot induced by various races and isolates have been identified in previous QTL mapping studies, suggesting that the *Ptr*-wheat system is more complex than just an inverse gene-for-gene model (Faris et al. 2013). Some QTL were race-nonspecific, contributing resistance to multiple races in bread wheat (Chu et al. 2008; Faris et al. 2012; Faris and Friesen 2005; Kariyawasam et al. 2016) and durum wheat (Chu et al. 2010).

Removal of the dominant susceptibility genes coupled with the introgression of other quantitative resistance loci should confer high and stable resistance to tan spot. Given the large number of identified QTL, it is prominent to remove redundancies and target major QTL in wheat breeding programs.

Meta-QTL analysis involves combining data from various mapping studies, and it can be useful for identification of redundant QTL, for candidate gene discovery, and for selecting major QTL for marker-assisted selection (MAS) in breeding applications (Goffinet and Gerber 2000). In meta-QTL analysis, a consensus linkage map is constructed based on individual linkage maps, and QTL identified from each study are projected onto the consensus map. Meta-QTL analysis can reduce a QTL to a smaller region to facilitate the discovery of the causal gene and enable the selection of more closely linked markers for effective MAS. Meta-QTL analysis can also estimate the global effect of a QTL region commonly identified from multiple populations and/or environments and prioritize the identified QTL for MAS (Yu et al. 2014; Maccaferri et al. 2015). Meta-QTL analysis has been conducted for Fusarium head blight resistance (Liu et al. 2009; Löffler et al. 2009; Venske et al. 2019), grain weight (Avni et al. 2018), leaf rust resistance (Soriano and Royo 2015), root-related traits (Soriano and Alvaro 2019), and stem rust resistance (Yu et al. 2014) in wheat, but not for tan spot resistance. In this study, a meta-QTL analysis of tan spot resistance was performed using results from previous mapping studies. We expect to obtain a deeper and broader understanding of the genetic basis of tan spot resistance in wheat and to prioritize meta-QTL for MAS in breeding.

Materials and methods

Construction of a consensus linkage map

R package "LP merge" (Endelman and Plomion 2014) was used to assemble an integrated map with three previously published consensus linkage maps (Somers et al. 2004; Marone et al. 2012; Maccaferri et al. 2014) and 21 individual linkage maps (Supplementary Table S1). The 21 individual linkage maps were derived from 21 mapping populations including 10 tetraploid wheat populations and 11 hexaploid wheat populations. Of the 21 mapping populations, 18 were previously employed for QTL mapping of tan spot resistance. The 21 populations are Attlia × CDC Go (ACDC, Zou et al. 2017), Altar × Langdon (AL, Virdi et al. 2016), BR34 × Grandin (BG, Faris and Friesen 2005), Ben × PI41025 (BP, Galagedara 2018), Calingiri × Wyalkatchem (CW, Shankar et al. 2017), Divide × PI272527 (DP527, Zhang et al. 2017), Ernie × Betavia (EB, Li et al. 2011), IGW2547 × Annuello (IA, Shankar et al. 2017), Joppa × 10Ae564 (Joppa10Ae,

Zhao et al. 2018), LMPG-6 × PI626573 (LP573, Liu et al. 2017), Louise × Penawawa (LP, Kariyawasam et al. 2016), Lebsock × PI94749 (LP749, Chu et al. 2010), MAGIC population (BMW, Stadlmeier et al. 2019), Rusty × Iumillo (RIum, Liu et al. 2019), Rusty × PI387336 (RP336, Liu et al. 2019), Rusty × PI387696 (RP696, Liu et al. 2019), Rusty × PI466979 (RP979, Liu et al. 2019), Rusty × PI183883 (Sharma et al. 2019), Sala-mouni × Katepwa (SK, Faris et al. 2012), TA4152-60 × ND495 (TN, Chu et al. 2008), and TA161-L1 × TAM105 (TT, Kalia et al. 2018). Brief information of the 21 linkage maps and mapping populations is listed in Supplementary Table S1.

Of the 21 linkage maps, 11 were constructed with SNP markers. However, seven were constructed with SNP markers genotyped using Illumina iSelect 9K, or 20K, or 90K arrays and four using genotype-by-sequencing (GBS). To better bridge SNP markers genotyped by different platforms across individual linkage maps, four tetraploid wheat populations (BP, DP527, Joppa10Ae, and RP883) originally genotyped with Illumina iSelect 9K or 90K SNP array were re-genotyped using GBS as described by Poland et al. (2012). A TASSEL-GBS pipeline was used for SNP discovery and genotype calling as described in Glaubitz et al. (2014). The *Triticum aestivum* IWGSC1.0 RefSeq v1.0 was used as a reference genome (Appels et al. 2018). The resultant GBS SNP markers were named based on their physical positions on the reference genome. SNP markers with more than 50% missing values were removed. Furthermore, SNP markers with segregation ratios exceeding 0.7:0.3 were considered distorted markers and therefore eliminated. We re-constructed the linkage maps using both Illumina iSelect array SNP markers and GBS SNP markers for the four mapping populations. The SNP markers were grouped for each mapping population using MSTmap (Wu et al. 2008) implemented in the R language package ASMap (Taylor and Butler 2015). For each linkage group, markers were ordered using Join-Map 4.0 (Van Ooijen 2006), and distances between markers were calculated using the Kosambi mapping function (Kosambi 1943).

The other 10 of the 21 individual linkage maps were constructed with DArT and/or SSR markers. Three previously published consensus maps built with SSR and/or DArT markers were included to increase connectivity among individual maps with SSR and/or DArT markers (Supplementary Table S2). The three previously published consensus maps were the 2004 Bread Wheat SSR Integrated map (Somers et al. 2004), the 2012 Durum Wheat SSR/DArT Integrated map (Marone et al. 2012), and the 2014 Durum Wheat SSR/DArT Integrated map (Maccaferri et al. 2014). They were assembled from six, six, and 12 individual linkage maps, respectively, none of which is same as any of the 21 individual mapping populations used in this study. The detailed

marker information of the 21 linkage maps and the resulted integrated map are listed in Supplementary Table S2.

To assess the quality of the resulted integrated map, we compared it to two other previously constructed wheat consensus maps (Wang et al. 2014; Maccaferri et al. 2015), where correlation of the shared marker order between the maps was calculated for each linkage group. In addition, the SNP markers mapped on the integrated linkage map were subjected to BLAST searches against the reference genome of *T. aestivum* IWGSC1.0 RefSeq v1.0 (Appels et al. 2018) to obtain their physical positions. The correlation of the mapped SNP marker orders between the integrated linkage map and physical position was calculated for each chromosome.

Collection of tan spot resistance loci identified in previous studies

Tan spot resistance loci were collected from 15 previous mapping studies that employed 18 mapping populations. Of the 18 mapping populations, eight were evaluated with isolates of race 1; twelve were evaluated with race 2 isolates; five were evaluated with race 3 isolates; six were evaluated with race 5 isolates; five were evaluated with locally collected isolates; and eight were evaluated for multiple *Ptr* races. No significant QTL associated with tan spot resistance was identified in the population RP979, for which only race 2 isolate 86-124 was evaluated (Liu et al. 2019). Among the remaining 17 populations, there were 135 QTL in total with LODs greater than 3.0 (Supplementary Table S3), which were used for further meta-QTL analysis.

To better organize the QTL identified from different studies, QTL were renamed according to the population they were identified in, the *Ptr* isolate and race associated with the QTL, growth stage, and the chromosomal location. Multiple QTL that mapped to the same linkage group from the same population and were associated with the same isolate(s) were distinguished by a number following the chromosome designation, e.g., BG_OH99(race3)_Seedling_3B.1 and BG_OH99(race3)_Seedling_3B.2, whereas QTL located on the same linkage group from the same population but detected in different environments or trials were distinguished by a unique letter following the chromosome designation, e.g., CW_Seedling_2A.a, CW_Booting_2A.b and CW_Seedling_2A.c. QTL associated with infection caused by uncharacterized local isolates were renamed based on the population name and chromosomal location. There were 29 QTL associated with resistance to race 1, 34 QTL associated with race 2, 12 QTL associated with race 3, and 13 QTL associated with race 5. There were 65 QTL mapped to the A sub-genome, 59 QTL mapped to the B sub-genome, and 11 QTL mapped to the D sub-genome. Chromosome 5A

possessed the highest number of QTL (22) and Chromosome 5D harbored a single QTL.

Meta-QTL analysis

Meta-QTL analysis was carried out using BioMercator V4.2 (Sosnowski et al. 2012). Individual QTL were first projected onto the resulted integrated map. Given N QTL projected on one linkage group, BioMercator tests five models assuming presence of 1-, 2-, 3-, 4-, or N-unique QTL, respectively. Akaike Information Criterion (AIC), an estimator of model fitting, was calculated and the model with the lowest AIC value was selected as the best model.

Candidate gene analysis on meta-QTL

All genes within the physical interval of each meta-QTL were first identified through surveying the annotation browser, where a total of 107,891 high-confidence protein-coding genes were annotated in the IWGSC RefSeq Annotation v1.0 (Appels et al. 2018). The genes retained after filtering with keyword "disease resistance" were considered as candidate genes and listed in the Supplementary Table S4.

Results

Construction of an integrated linkage map

An integrated linkage map was assembled from 21 individual linkage maps and three previously published consensus maps. The integrated linkage map contained 47,309 markers, including 2998 DArT, 38,231 SNP, 3034 SSR, and 3046 other types of markers such as AFLP, STS, and TRAP (Supplementary Table S2). The total length is 4,080.5 cM, with a range of 104.0 cM to 409.5 cM across the 21 linkage groups (Table 1). For the linkage groups from the A and B sub-genome, marker densities ranged from 8.4 to 15.0 markers per cM (Table 1). The densities for the seven linkage groups from the D sub-genome were much lower, ranging from 0.7 to 1.7 markers per cM (Table 1), because all 11 hexaploid wheat individual linkage maps were constructed with mainly SSR or DArT markers and without the benefit of high-density SNP markers.

To assess the quality of the integrated linkage map, common markers mapped on the same linkage group were

Table 1 Information of the integrated linkage map and its correlations of common marker orders with previously published consensus maps and physical positions

Consensus map	Markers (no.)	Length (cM)	Marker density[a]	Order correlation[b]	Order correlation[c]	Order correlation[d]
1A	3083	281.2	11.0	0.97	0.99	0.99
1B	3344	252.8	13.2	0.98	0.99	0.99
2A	3237	259.6	12.5	0.94	0.98	0.99
2B	4052	312.5	13.0	0.98	0.98	0.99
3A	2822	271.0	10.4	0.99	0.97	0.99
3B	3834	255.7	15.0	0.95	0.96	0.99
4A	2770	285.2	9.7	0.96	0.96	0.98
4B	1768	211.4	8.4	0.97	0.98	0.98
5A	2595	201.0	12.9	0.96	0.98	0.99
5B	3639	317.8	11.4	0.99	0.99	0.99
6A	2820	233.9	12.1	0.96	0.95	0.98
6B	4041	310.8	13.0	0.97	0.99	0.99
7A	3718	409.5	9.1	0.95	0.96	0.99
7B	3563	370.7	9.6	0.99	0.99	0.98
1D	328	212.0	1.5	–	–	–
2D	432	249.4	1.7	–	–	–
3D	245	347.9	0.7	–	–	–
4D	128	104.0	1.2	–	–	–
5D	281	256.5	1.1	–	–	–
6D	298	206.8	1.4	–	–	–
7D	311	290.7	1.1	–	–	–

[a]Number of markers per cM

[b]Order correlation between the integrated linkage map and the consensus map in Wang et al. (2014)

[c]Order correlation between the integrated linkage map and the consensus map in Maccaferri et al. (2015)

[d]Oder correlation between the integrated linkage map and physical position

used to calculate the correlations of the marker orders between our integrated map and two previously published consensus maps, one in tetraploid wheat (Maccaferri et al. 2015) and the other in hexaploid wheat (Wang et al. 2014). The correlations ranged from 0.94 to 0.99 across the 14 linkage groups of A and B sub-genomes (Table 1), indicating high synteny between our integrated map and previously published consensus maps. Because the 11 hexaploid individual linkage maps used to construct our integrated map lacked SNP markers while the hexaploid consensus map from Wang et al. (2014) was constructed solely with SNP markers (genotyped by Illumina iSelect 90K array), few markers on the D sub-genome were shared between our integrated map and the consensus map from Wang et al. (2014). For that reason, no correlations were estimated for the D sub-genome linkage groups.

Meta-QTL analysis

Out of the 135 QTL identified from 17 mapping populations, 129 were successfully projected onto the integrated linkage map (Supplementary Table S3). Of the 129 QTL projected to the integrated linkage map, 23 remained as single QTL, and the other 106 QTL were grouped into 20 meta-QTL. One meta-QTL on chromosome 6A consisted of two initial QTL identified from the EB population in two independent greenhouse trials (Li et al. 2011), and was determined upon further analysis to not be a meta-QTL. The remaining 19 meta-QTL were located on chromosomes 1A, 1B, 2A, 2B, 2D, 3A, 3B, 4A, 5A, 5B, 7A, and 7B (Fig. 1, Table 2). Initial QTL of 15 meta-QTL were identified from multiple populations (Table 2); initial QTL of the other four meta-QTL were identified in only one population but showing resistance to multiple races (Table 2). The number of clustered QTL per meta-QTL ranged from two to 13 (Table 2). The genetic position, genetic interval, physical interval, and other related information for each meta-QTL are listed in Table 2.

The two meta-QTL detected on chromosome 1A, MQTL-1A.1 and MQTL-1A.2, are likely co-localized with *Tsc1*. The MQTL-1A.1 comprises seven initial QTL identified from three hexaploid common wheat mapping populations, IA, LP, and TT, conferring susceptibility to isolates of races 1 and 3, AR CrossB10, and Australia local isolates (Table 2 and Supplementary Table S3). Both races 1 and 3 produce Ptr ToxC. AR CrossB10 is an unclassified isolate (Ali et al. 2010) but likely produces Ptr ToxC because it can cause extensive chlorosis on Ptr ToxC susceptible check 6B365 (Kariyawasam et al. 2016). The initial QTL identified from LP were believed to be *Tsc1,* based on its significant associations with Ptr ToxC-producing isolates but not with races 2 and 5 (Kariyawasam et al. 2016). Similar region was identified to confer susceptibility to infiltration of partially purified Ptr ToxC (Effertz et al. 2002). MQTL-1A.2 comprises

six initial QTL identified from three hexaploid common wheat mapping populations, LP573, EB and BMW. The initial QTL identified in LP573 was proposed to be *Tsc1* due to its association with Ptr ToxC-producing isolates only (Liu et al. 2017). There may be a structural variant or multiple copies of *Tsc1* on chromosome arm 1AS, and both MQTL-1A.1 and MQTL-1A.2 contain the gene *Tsc1*. Differences on population size, marker density, and significance thresholds used in individual QTL mapping studies can result in varied confidence intervals, which can further affect the meta-QTL determination. Given experimental limitations, it is also possible that MQTL-1A.1 and MQTL-1A.2 are one locus but were identified as two meta-QTL.

MQTL-2B comprises five initial QTL identified from two hexaploid common wheat populations AL and EB, and one tetraploid wheat population RP336 (Fig. 1 and Table 2), and is likely co-localized with *Tsc2*. Reaction to Ptr ToxB infiltration suggests that the initial QTL identified from AL population was *Tsc2* (Virdi et al. 2016). Abeysekara et al. (2010) finely mapped *Tsc2* and developed a diagnostic marker XBE444541. The marker XBE444541 was mapped near ~24.1 Mbp on chromosome 2B. This evidence indicates the co-localization of MQTL-2B with *Tsc2*. However, the initial QTL identified in the RP336 population confers resistance to race 2 isolate 86-124, which does not produce Ptr ToxB (Liu et al. 2019). In addition, the population EB was tested using infected straws with Australian local isolates (Li et al. 2011), from which Ptr ToxB was rarely produced. Therefore, it is possible that MQTL-2B is composed of an additional gene conferring resistance/susceptibility to NEs other than Ptr ToxB (Liu et al. 2019).

MQTL-5B.2 consists of eight initial QTL identified from three hexaploid wheat mapping populations LP573, SK, and TN, conferring resistance to races 1 and 2, both producing Ptr ToxA (Table 2). LP573 was evaluated for races 1, 2, 3, and 5, but this QTL region was detected only for Ptr ToxA-producing isolates (Liu et al. 2017). Reaction to infiltration of purified Ptr ToxA was conducted on the LP573 population as well and the result indicated that the identified QTL co-localizes with *Tsn1* (Liu et al. 2017).

Five meta-QTL (MQTL-1B, MQTL-2A.2, MQTL-3B.2, MQTL-5A.2, and MQTL-5B.1) are likely race non-specific because they confer resistance to multiple races. MQTL_2A.2 comprises 13 initial QTL identified from three hexaploid common wheat mapping populations CW, LP573, and TN, conferring resistance to races 1, 2, 3, 5, and uncharacterized local isolates from Australia (Fig. 1, Table 2, and Supplementary Table S3). The seven initial QTL identified in the CW population conferred resistance to Australian local isolates under varied environments and growth stages (Supplementary Table S3; Shankar et al. 2017). The four initial QTL identified in the TN population conferred resistance to races 1, 2, 3, and 5 (Supplementary Table S3; Chu et al. 2008). The two initial QTL
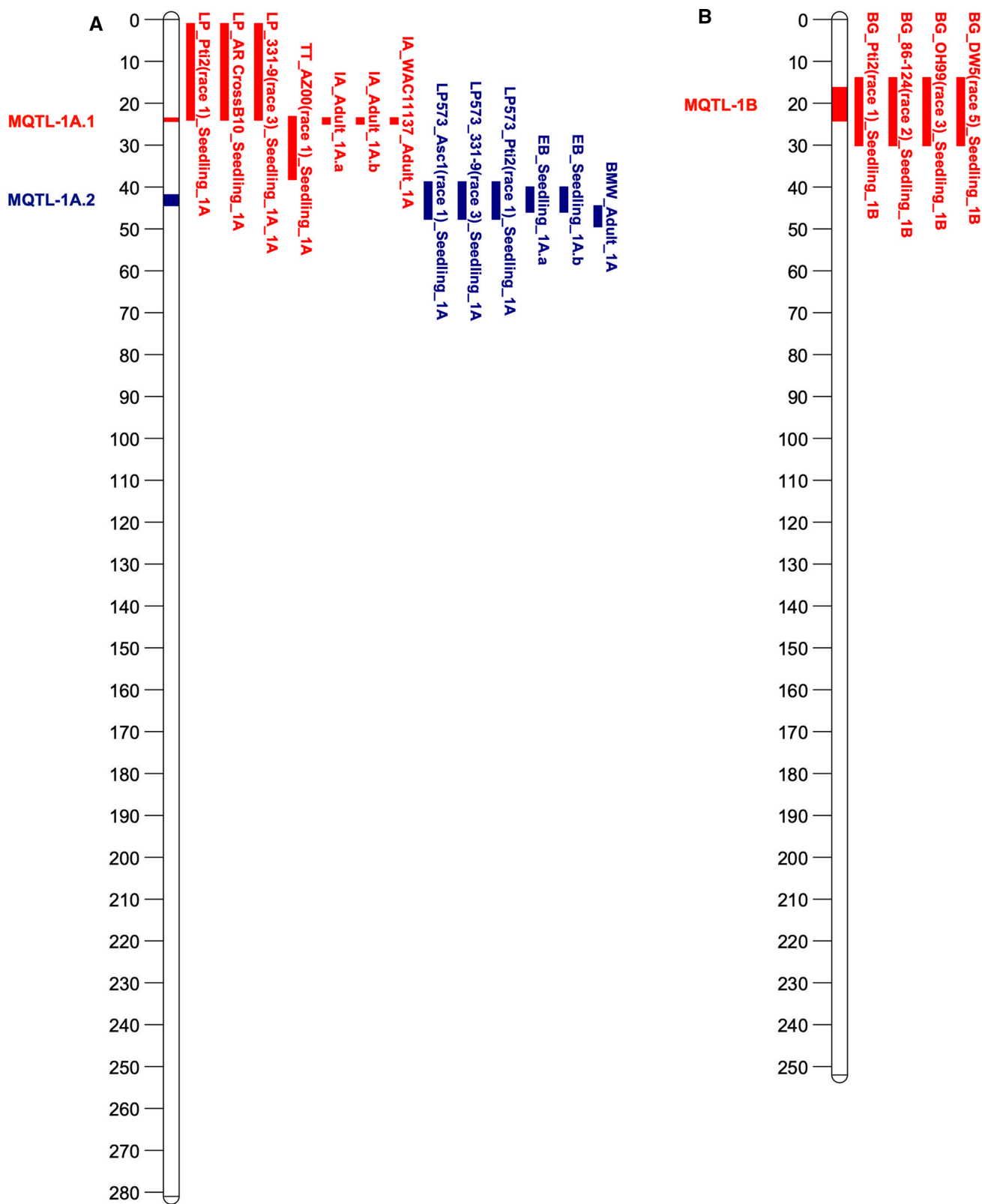
Fig. 1 Tan spot resistance meta-QTL and initial QTL projected on the integrate linkage map in wheat. Meta-QTL is represented by a bar with red or blue color on the chromosome. An initial QTL is represented by a bar with red or blue color on the right side of the chromosome. On each chromosome, a meta-QTL and its initial QTL are marked with a same color (color figure online)

Table 2 Summary of the identified meta-QTL for tan spot resistance

Meta-QTL	Genetic position (cM)	95% genetic interval (cM)	Physical interval[a] (Mbp)	Average LOD	Average R^2 (%)	Initial QTL
MQTL-1A.1	24.0	23.5–24.4	3.4–9.4	10.8	18.2	LP_Pti2(race 1)_Seedling_1A
						LP_AR CrossB10_Seedling_1A
						LP_331-9(race 3)_Seedling_1A
						TT_AZ00(race 1)_Seedling_1A
						IA_Adult_1A.a
						IA_Adult_1A.b
						IA_WAC11137_Adult_1A
MQTL-1A.2	43.1	41.8–44.5	7.3–12.1	9.3	19.3	LP573_Asc1(race 1)_Seedling_1A
						LP573_Pti2(race 1)_Seedling_1A
						LP573_331-9(race 3)_Seedling_1A
						EB_Seedling_1A.a
						EB_Seedling_1A.b
						BMW_Adult_1A
MQTL-1B	20.3	16.2–24.3	3.6–6.3	7.0	20.8	BG_Pti2(race 1)_Seedling_1B
						BG_86-124(race 2)_Seedling_1B
						BG_OH99(race 3)_Seedling_1B
						BG_DW5(race 5)_Seedling_1B
MQTL-2A.1	70.7	69.1–72.2	45.1–58.7	7.5	20.1	CW_Seedling_2A.a
						BMW_Adult_2A
MQTL-2A.2	84.1	82.3–84.9	65.7–262.1	6.0	17.4	TN_Pti2(race 1)_Seedling_2A
						TN_86-124(race 2)_Seedling_2A
						TN_OH99(race 3)_Seedling_2A
						TN_DW5(race 5)_Seedling_2A
						LP573_Asc1(race 1)_Seedling_2A
						LP573_DW5(race 5)_Seedling_2A
						CW_Booting_2A.b
						CW_Seedling_2A.c
						CW_Adult_2A.d
						CW_Adult_2A.e
						CW_WAC11137_Adult_2A.a
						CW_WAC11137_Adult_2A.b
						CW_WAC11137_Adult_2A.c
MQTL-2B	58.3	54.6–62.1	1.2–27.2	7.2	27.4	EB_Seedling_2B.a
						EB_Seedling_2B.b
						EB_Seedling_2B.c
						RP336_86-124(race 2)_Seedling_2B
						AL_DW5(race 5)_Seedling_2B
MQTL-2D	156.0	155.6–156.4	312.3–383.0	6.3	6.0	LP_Pti2(race 1)_Seedling_2D
						LP_86-124(race 2)_Seedling_2D
						LP_AR CrossB10_Seedling_2D
						LP_331-9(race 3)_Seedling_2D
MQTL-3A	35.2	33.0–37.5	20.0–21.8	5.1	10.1	RP336_86-124ΔToxA(race 2)_ Seedling_3A
						RP696_86-124(race 2)_Seedling_3A
						RIum_86-124(race 2)_Seedling_3A
						LP749_Pti2(race 1)_Seedling_3A
						LP749_86-124(race 2)_Seedling_3A
MQTL-3B.1	45.5	42.6–48.5	23.9–68.8	5.2	19.2	BG_OH99(race 3)_Seedling_3B.1

Table 2 (continued)

Meta-QTL	Genetic position (cM)	95% genetic interval (cM)	Physical interval[a] (Mbp)	Average LOD	Average R^2 (%)	Initial QTL
MQTL-3B.2	62.8	59.4–66.1	465.2–583.4	17.0	27.0	EB_Seedling_3B
						LP_86-124(race 2)_Seedling_3B
						LP_AR CrossB10_Seedling_3B
						LP_DW5(race 5)_Seedling_3B
						LP_Pti2(race 1)_Seedling_3B
						LP_331-9(race 3)_Seedling_3B
						LP749_Pti2(race 1)_Seedling_3B
						LP749_86-124(race 2)_Seedling_3B
						BG_Pti2(race 1)_Seedling_3B
						BG_86-124(race 2)_Seedling_1B
						BG_OH99(race 3)_Seedling_3B.2
						BG_DW5(race 5)_Seedling_3B
MQTL-5A.1	88.5	81.1–95.9	437.4–482.1	4.5	13.0	RP696_86-124(race 2)_Seedling_5A.1
						RP336_86-124(race 2)_Seedling_5A.1
						LP749_Pti2(race 1)_Seedling_5A.1
						LP749_86-124(race 2)_Seedling_5A.1
MQTL-5A.2	139.9	138.9–141.8	592.1–614.4	7.3	10.8	BP_DW5(race 5)_Seedling_5A
						BP_86-124(race 2)_Seedling_5A
						BP_Pti2(race 1)_Seedling_5A
						BP_AR CrossB10_Seedling_5A
						BP_331-9(race 3)_Seedling_5A
						LP_86-124(race 2)_Seedling_5A
						LP_Pti2(race 1)_Seedling_5A
						LP_DW5(race 5)_Seedling_5A
						LP_AR CrossB10_Seedling_5A
						LP_331-9(race 3)_Seedling_5A
						TN_Pti2(race 1)_Seedling_5A
						TN_86-124(race 2)_Seedling_5A
						TN_DW5(race 5)_Seedling_5A
MQTL-5A.3	174.3	172.9–175.8	671.3–676	8.8	16.2	RP696_86-124(race 2)_Seedling_5A.2
						RP336_86-124(race 2)_Seedling_5A.2
						RP336_86-124ΔToxA(race 2)_Seedling_5A
						LP749_Pti2(race 1)_Seedling_5A.2
						LP749_86-124(race 2)_Seedling_5A.2
MQTL-5B.1	80.0	74.5–85.5	58.8–448	7.4	21.0	TN_Pti2(race 1)_Seedling_5B.1
						TN_86-124(race 2)_Seedling_5B.1
						TN_OH99(race 3)_Seedling_5B
						TN_DW5(race 5)_Seedling_5B
MQTL-5B.2	123.8	120.4–125.6	541.7–549.9	10.8	21.5	TN_Pti2(race 1)_Seedling_5B.2
						TN_86-124(race 2)_Seedling_5B.2
						SK_Pti2(race 1)_Seedling_5B
						SK_86-124(race 2)_Seedling_5B
						LP573_Asc1(race 1)_Seedling_5B
						LP573_Pti2(race 1)_Seedling_5B
						LP573_86-124(race 2)_Seedling_5B
MQTL-5B.3	167.5	164.7–170.7	663.1–679.4	3.9	12.9	EB_Seedling_5B.a
						EB_Seedling_5B.b

Table 2 (continued)

Meta-QTL	Genetic position (cM)	95% genetic interval (cM)	Physical interval[a] (Mbp)	Average LOD	Average R^2 (%)	Initial QTL
						LP573_DW5(race 5)_Seedling_5B
MQTL-7A	113.6	111.7–115.6	116.1–133.6	5.5	11.3	SK_Pti2(race 1)_Seedling_7B
						SK_86-124(race 2)_Seedling_7B
MQTL-7B.1	80.4	78.4–82.4	21.0–34.0	3.9	6.3	SK_AR LonB2_Seedling_7B
						LP749_Pti2(race 1)_Seedling_7B
						LP749_86-124(race 2)_Seedling_7B
MQTL-7B.2	171.8	170.1–172.1	614.2–622.8	4.2	10.6	IA_Adult_7B
						CW_Booting_7B
						LP_Pti2(race 1)_Seedling_1A
						LP_AR CrossB10_Seedling_1A

[a]Physical interval was estimated by physical positions of the adjacent SNP markers

found in population LP573 conferred resistance to races 1 and 3 (Liu et al. 2017). The LP573 population was also evaluated for resistance to isolates of races 2 and 5, but no significant resistance was identified in this region (Liu et al. 2017). The lack of resistance to races 2 and 5 in LP573 could be due to epistatic interaction of MQTL-2A.2 with other loci in LP573. In addition, MQTL-2A.1 and MQTL-2A.2 could be a single locus, because their initial QTL were overlapping (Fig. 1 and Table 2) and both meta-QTL comprised initial QTL identified from the CW population but at different environments.

Candidate gene analysis

No disease resistance-related candidate genes were identified for MQTL-5A.3, MQTL-5B.2, and MQTL-7B.2 (Supplementary Table S4). Lack of candidate genes for MQTL-5B.2, which is co-localized with *Tsn1* that confers susceptibility to Ptr ToxA, can be explained by the fact that Chinese Spring (CS) is insensitive to Ptr ToxA, suggesting no *Tsn1* gene present in the reference genome. For the other 16 meta-QTL, two to 85 candidate genes were found inside their physical intervals. Most of the candidate genes were NBS- and/or LRR-like proteins (Supplementary Table S4). There were 85 candidate genes for MQTL-2B, which is co-localized with *Tsc2* that confers susceptibility to Ptr ToxB. However, CS is insensitive to Ptr ToxB and therefore none of the 85 genes would be *Tsc2*. Several powdery mildew resistance genes were found in the interval of MQTL-1A.1 and MQTL-1B (Supplementary Table S4).

Discussion

Genetic architecture of tan spot resistance revealed by meta-QTL analysis

To gain a better understanding of the genetic architecture of tan spot resistance, we performed meta-QTL analysis using reported QTL from previous mapping studies. In total, 129 QTL identified from 17 mapping populations in 15 previous QTL mapping studies were projected onto the integrated linkage map. Out of the 129 projected QTL, 104 were grouped into 19 meta-QTL, suggesting that a majority of the previously mapped tan spot resistance loci were shared by multiple populations and/or showed resistance to multiple races/isolates.

Three known Ptr NE-wheat interactions including Ptr ToxA-*Tsn1*, Ptr ToxB-*Tsc2*, and Ptr ToxC-*Tsc1* have been characterized. MQTL-1A.1 and/or MQTL-1A.2 co-localized with *Tsc1*, MQTL-2B co-localized with *Tsc2*, and MQTL-5B.2 co-localized with *Tsn1*. Per initial QTL studies, the three genes showed varied disease effects across mapping populations (Table 2; Chu et al. 2008; Faris et al. 2012; Liu et al. 2017). In addition to environment and genotype-by-environment interactions, complex genetic architecture could partially explain the varied effects of the three genes detected in different studies. For example, *Tsn1* was detected as a QTL in some hexaploid bread wheat mapping populations (Chu et al. 2008; Faris et al.

2012; Kariyawasam et al. 2018; Liu et al. 2017), but not others (Faris and Friesen 2005). Evaluation of Australian bread wheat varieties suggested that the importance of Ptr ToxA-*Tsn1* interaction in tan spot development depended upon the wheat genetic background (See et al. 2018). Regarding tetraploid wheat, eight mapping populations were evaluated with races 1 and/or 2 in one of our previous studies (Chu et al. 2010; Virdi et al. 2016; Liu et al. 2019), but none of them showed that *Tsn1* was significantly associated with disease, even among the five populations segregating for *Tsn1*. It was proposed that some non-race specific QTL might work upstream of the Ptr ToxA-*Tsn1* interaction precluding the development of tan spot (Kariyawasam et al., 2016), which may explain the lack of significance of *Tsn1* in those populations.

Five meta-QTL, MQTL-1B, MQTL-2A.2, MQTL-2D, MQTL-3B.2, MQTL-5A.2, and MQTL-5B.1, comprised of 46 initial QTL, confer resistance to multiple races and are likely race non-specific. The initial QTL of MQTL-2A.2 conferred resistance to tan spot not only at the seedling stage under controlled environments, but also at tillering and adult stages in a field trial (Shankar et al. 2017). Most previous studies were conducted at the seedling stage under controlled environments. It would be beneficial to test if other race-nonspecific meta-QTL conferred resistance at other growth stages under field conditions. Likewise, it is also crucial to map putative novel loci at varied growth stages under field conditions.

MQTL-3A, MQTL-5A.1, and MQTL-5A.3, comprised of 14 initial QTL, were identified from four tetraploid wheat mapping populations including LP749, RP336, RP696, and RIum. The four tetraploid wheat mapping populations were only evaluated for resistance to races 1 and 2 (Chu et al. 2010; Liu et al. 2019), both of which produce Ptr ToxA. The 11 hexaploid wheat mapping populations used for meta-QTL analysis were evaluated with multiple races, none of which possessed QTL in these three meta-QTL regions. Therefore, it is possible that those loci are specific to tetraploid wheat. The desirable resistance alleles of the three meta-QTL were from the parents Rusty and Lebsock, both of which are sensitive to Ptr ToxA but highly resistant to races 1 and 2. Therefore, it will be meaningful to test if those meta-QTL also confer race-nonspecific resistance by screening resistance to other races on the four mapping populations.

Identification of co-localized QTL from the studies not included in meta-QTL analysis

In addition to the 15 mapping studies, some other previously published QTL mapping studies were not used for the meta-QTL analysis due to lack of detailed information of the identified QTL or lack of sufficient common markers between the individual linkage map and our integrated linkage map

(Supplementary Table S5). To identify QTL not included in meta-QTL analysis that potentially co-localized with the identified meta-QTL, the closely linked markers to the QTL in question were aligned to the same reference genome *T. aestivum* IWGSC1.0 RefSeq v1.0 (Appels et al. 2018). Sun et al. (2010) identified a locus associated with resistance to the race 1 isolate AZ-00, from which the closely linked marker *Xcfa2153* was aligned to ~7.2 Mbp on chromosome 1A (Supplementary Table S5) and located in the physical interval of the MQTL-1A.1. Abeysekara et al. (2010) finely mapped *Tsc2* and developed the diagnostic marker *XBE444541*, which mapped near ~24.1 Mbp on chromosome 2B and co-localized with MQTL-2B (Supplementary Table S5). QTL identified from five association studies conducted in hexaploid wheat (Dinglasan et al. 2019; Liu et al. 2015; Patel et al. 2013; Perez-Lara et al. 2017; Singh et al. 2016) were co-localized with MQTL-1A.1, MQTL-1A.2, MQTL-1B, MQTL-2B, MQTL-3B.2, MQTL-5B.2, and MQTL-5B.3 (Supplementary Table S6). Interestingly, in one of the five association studies (Perez-Lara et al. 2017), Ptr ToxB infiltration reaction using 83 Canadian spring wheat cultivars found two QTL, one located on chromosome 2B and co-localized with the MQTL-2B (*Tsc2*) and the other located on chromosome 5B and co-localized with the MQTL-5B.3. One of the initial QTL from MQTL-5B.3 identified in the population LP573 conferred resistance to race 5 isolate DW5 producing Ptr ToxB (Liu et al. 2017), indicating that MQTL-5B.3 may cover a novel gene that also confers resistance or susceptibility to Ptr ToxB. The fact that Ptr ToxB is associated with two loci conflicts with the inverse gene-for-gene model proposed for the interaction between wheat and Ptr NEs. Further studies on *Tsc2* and the causal gene within MQTL-5B.3 are needed to elucidate the underling mechanism.

Implication of MAS for breeding tan spot resistance in wheat

Introgression of desirable alleles of major QTL through MAS is an effective and efficient approach toward improvement of a quantitative trait like tan spot resistance in wheat. Meta-QTL analysis could identify redundant QTL and prioritize QTL for MAS. Ideally, the preferred criteria of meta-QTL for MAS are large effect, a small confidence interval, and high number of initial QTL identified from diverse populations (Löffler et al. 2009). Removal of the three dominant susceptibility tan spot genes from a breeding population is highly recommended, although they played a major role only in some populations and some genotypes. In addition to the three susceptibility genes, our meta-QTL analysis revealed three race-nonspecific meta-QTL including MQTL_2A.2, MQTL_3B.2, and MQTL_5A.2 that also meet the preferred criteria mentioned earlier. Integrating desirable

alleles of those race-nonspecific meta-QTL could provide high and stable tan spot resistance induced by varied races and isolates. Of them, MQTL-3B.2 conferred resistance in both hexaploid bread wheat and tetraploid wheat. Association mapping using 371 durum wheat collections revealed markers in this region (ca. 466.6–474.3 Mbp) significantly associated with resistance to races 1, 2, 3, and 5 (Liu et al. unpublished data). We have also checked the NDSU durum wheat breeding material, and none of the released cultivars or breeding lines from 2012 to 2018 advanced yield trials have the desirable allele of MQTL-3B.2 (Li et al. unpublished data). The rare frequency of the desirable allele implicates great potential toward the improvement of tan spot resistance in the NDSU durum wheat breeding population. Developing diagnostic markers for the MQTL-3B.2 will facilitate introgression of the desirable allele into the NDSU durum wheat breeding population through MAS. Further validation of the three race-nonspecific meta-QTL in an active breeding population under field conditions is essential for establishing the systematic application for MAS in a breeding program.

Compliance with ethical standards

References

Abeysekara NS, Friesen TL, Liu Z, McClean PE, Faris JD (2010) Marker development and saturation mapping of the tan spot Ptr ToxB sensitivity locus *Tsc2* in hexaploid wheat. Plant Genome 3:179–189. https://doi.org/10.3835/plantgenome2010.07.0017

Ali S, Gurung S, Adhikari TB (2010) Identification and characterization of novel isolates of *Pyrenophora tritici-repentis* from Arkansas. Plant Dis 94:229–235

Appels R, Eversole K, Feuillet C, Keller B, Rogers J, Stein N, Pozniak CJ, Choulet F, Distelfeld A, Poland J (2018) Shifting the limits in wheat research and breeding using a fully annotated reference genome. Science 361:eaa7191

Avni R, Oren L, Shabtai G, Assili S, Pozniak C, Hale I, Ben-David R, Peleg Z, Distelfeld A (2018) Genome based meta-QTL analysis of grain weight in tetraploid wheat identifies rare alleles of GRF4 associated with larger grains. bioRxiv. https://doi.org/10.1101/415240

Bhathal J, Loughman R, Speijers J (2003) Yield reduction in wheat in relation to leaf disease from yellow (tan) spot and septoria nodorum blotch. Eur J Plant Pathol Dordr 109:435–443. https://doi.org/10.1023/A:1024277420773

Chu CG, Friesen TL, Xu SS, Faris JD (2008) Identification of novel tan spot resistance loci beyond the known host-selective toxin insensitivity genes in wheat. Theor Appl Genet 117:873–881. https://doi.org/10.1007/s00122-008-0826-z

Chu CG, Chao S, Friesen TL, Faris JD, Zhong S, Xu SS (2010) Identification of novel tan spot resistance QTLs using an SSR-based linkage map of tetraploid wheat. Mol Breed 25:327–338. https://doi.org/10.1007/s11032-009-9335-2

Ciuffetti LM, Manning VA, Martinez JP, Pandelova I, Andrie RM (2003) Proteinaceous toxins of *Pyrenophora tritici-repentis* and investigation of the site-of-action of Ptr ToxA. In: Rasmussen JB, Friesen TL, Ali S (eds) Proceedings of the fourth international wheat tan spot and spot blotch workshop. North Dakota Agricultural Experiment Station, Fargo, pp 96–102

Ciuffetti LM, Manning VA, Pandelova I, Betts MF, Martinez JP (2010) Host-selective toxins, Ptr ToxA and Ptr ToxB, as necrotrophic effectors in the *Pyrenophora tritici-repentis*-wheat interaction: research review. New Phytol 187:911–919. https://doi.org/10.1111/j.1469-8137.2010.03362.x

Dinglasan EG, Singh D, Shankar M, Afanasenko O, Platz G, Godwin ID, Voss-Fels KP, Hickey LT (2019) Discovering new alleles for yellow spot resistance in the Vavilov wheat collection. Theor Appl Genet 132:149–162. https://doi.org/10.1007/s00122-018-3204-5

Effertz RJ, Meinhardt SW, Anderson JA, Jordahl JG, Francl LJ (2002) Identification of a chlorosis-inducing toxin from *Pyrenophora tritici-repentis* and the chromosomal location of an insensitivity locus in wheat. Phytopathology 92:527–533. https://doi.org/10.1094/PHYTO.2002.92.5.527

Endelman JB, Plomion C (2014) LPmerge: an R package for merging genetic maps by linear programming. Bioinformatics 30:1623–1624. https://doi.org/10.1093/bioinformatics/btu091

Faris JD, Friesen TL (2005) Identification of quantitative trait loci for race-nonspecific resistance to tan spot in wheat. Theor Appl Genet 111:386–392. https://doi.org/10.1007/s00122-005-2033-5

Faris JD, Zhang Z, Lu H, Lu S, Reddy L, Cloutier S, Fellers JP, Meinhardt SW, Rasmussen JB, Xu SS, Oliver RP, Simons KJ, Friesen TL (2010) A unique wheat disease resistance-like gene governs effector-triggered susceptibility to necrotrophic pathogens. Proc Natl Acad Sci 107:13544–13549. https://doi.org/10.1073/pnas.1004090107

Faris JD, Abeysekara NS, McClean PE, Xu SS, Friesen TL (2012) Tan spot susceptibility governed by the *Tsn1* locus and race-nonspecific resistance quantitative trait loci in a population derived from the wheat lines Salamouni and Katepwa. Mol Breed 30:1669–1678. https://doi.org/10.1007/s11032-012-9750-7

Faris JD, Liu Z, Xu SS (2013) Genetics of tan spot resistance in wheat. Theor Appl Genet 126:2197–2217. https://doi.org/10.1007/s00122-013-2157-y

Friesen TL, Faris JD (2004) Molecular mapping of resistance to *Pyrenophora tritici-repentis* race 5 and sensitivity to Ptr ToxB in wheat. Theor Appl Genet 109:464–471

Galagedara NN (2018) Identification of quantitative trait loci for resistance to tan spot in durum wheat. North Dakota State University

Glaubitz JC, Casstevens TM, Lu F, Harriman J, Elshire RJ, Sun Q, Buckler ES (2014) TASSEL-GBS: a high capacity genotyping by sequencing analysis pipeline. PLoS ONE 9:e90346. https://doi.org/10.1371/journal.pone.0090346

Goffinet B, Gerber S (2000) Quantitative trait loci: a meta-analysis. Genetics 155:463–473

Guo J, Shi G, Liu Z (2018) Characterizing Virulence of the *Pyrenophora tritici-repentis* isolates lacking both ToxA and ToxB genes. Pathogens 7:74

Kalia B, Bockus WW, Singh S, Tiwari VK, Gill BS (2018) Mapping of quantitative trait loci for resistance to race 1 of *Pyrenophora*

tritici-repentis in synthetic hexaploid wheat. Plant Breed 137:313–319. https://doi.org/10.1111/pbr.12586

Kariyawasam GK, Carter AH, Rasmussen JB, Faris J, Xu SS, Mergoum M, Liu Z (2016) Genetic relationships between race-nonspecific and race-specific interactions in the wheat–*Pyrenophora tritici-repentis* pathosystem. Theor Appl Genet 129:897–908. https://doi.org/10.1007/s00122-016-2670-x

Kariyawasam GK, Hussain W, Easterly A, Guttieri M, Belamkar V, Poland J, Venegas J, Baenziger S, Marais F, Rasmussen JB, Liu Z (2018) Identification of quantitative trait loci conferring resistance to tan spot in a biparental population derived from two Nebraska hard red winter wheat cultivars. Mol Breed 38(11):140. https://doi.org/10.1007/s11032-018-0901-3

Kosambi DD (1943) The estimation of map distances from recombination values. Ann Eugen 12:172–175. https://doi.org/10.1111/j.1469-1809.1943.tb02321.x

Li HB, Yan W, Liu GR, Wen SM, Liu CJ (2011) Identification and validation of quantitative trait loci conferring tan spot resistance in the bread wheat variety Ernie. Theor Appl Genet 122:395–403. https://doi.org/10.1007/s00122-010-1455-x

Liu S, Hall MD, Griffey CA, McKendry AL (2009) Meta-analysis of QTL associated with Fusarium head blight resistance in wheat. Crop Sci 49:1955–1968

Liu Z, El-Basyoni I, Kariyawasam G, Zhang G, Fritz A, Hansen J, Marais F, Friskop A, Chao S, Akhunov E, Baenziger PS (2015) Evaluation and association mapping of resistance to tan spot and *Stagonospora nodorum* blotch in adapted winter wheat germplasm. Plant Dis 99:1333–1341. https://doi.org/10.1094/PDIS-11-14-1131-RE

Liu Z, Zurn JD, Kariyawasam G, Faris JD, Shi G, Hansen J, Rasmussen JB, Acevedo M (2017) Inverse gene-for-gene interactions contribute additively to tan spot susceptibility in wheat. Theor Appl Genet 130:1267–1276. https://doi.org/10.1007/s00122-017-2886-4

Liu Y, Zhang Q, Salsman E, Fiedler JD, Hegstad JB, Liu Z, Faris JD, Xu SS, Li X (2019) QTL mapping of resistance to tan spot induced by race 2 of *Pyrenophora tritici-repentis* in tetraploid wheat. Theor Appl Genet. https://doi.org/10.1007/s00122-019-03474-2

Löffler M, Schön C-C, Miedaner T (2009) Revealing the genetic architecture of FHB resistance in hexaploid wheat (*Triticum aestivum* L.) by QTL meta-analysis. Mol Breed 23:473–488. https://doi.org/10.1007/s11032-008-9250-y

Maccaferri M, Cane M, Sanguineti MC, Salvi S, Colalongo MC, Massi A, Clarke F, Knox R, Pozniak CJ, Clarke JM, Fahima T, Dubcovsky J, Xu S, Ammar K, Karsai I, Vida G, Tuberosa R (2014) A consensus framework map of durum wheat (*Triticum durum* Desf.) suitable for linkage disequilibrium analysis and genome-wide association mapping. BMC Genom 15:873. https://doi.org/10.1186/1471-2164-15-873

Maccaferri M, Ricci A, Salvi S, Milner SG, Noli E, Martelli PL, Casadio R, Akhunov E, Scalabrin S, Vendramin V, Ammar K, Blanco A, Desiderio F, Distelfeld A, Dubcovsky J, Fahima T, Faris J, Korol A, Massi A, Mastrangelo AM et al (2015) A high-density, SNP-based consensus map of tetraploid wheat as a bridge to integrate durum and bread wheat genomics and breeding. Plant Biotechnol J 13:648–663. https://doi.org/10.1111/pbi.12288

Manning VA (2005) Localization of Ptr ToxA produced by *Pyrenophora tritici-repentis* reveals protein import into wheat mesophyll cells. Plant Cell 17:3203–3212. https://doi.org/10.1105/tpc.105.035063

Marone D, Laidò G, Gadaleta A, Colasuonno P, Ficco DBM, Giancaspro A, Giove S, Panio G, Russo MA, De Vita P, Cattivelli L, Papa R, Blanco A, Mastrangelo AM (2012) A high-density consensus map of A and B wheat genomes. Theor Appl Genet 125:1619–1638. https://doi.org/10.1007/s00122-012-1939-y

Meinhardt SW, Ali S, Ling H, Francl LJ (2003) A new race of *Pyrenophora tritici-repentis* that produces a putative host-selective toxin. In: Rasmussen JB, Friesen TL, Ali S (eds) Proceedings of the fourth international wheat tan spot and spot blotch workshop. North Dakota Agricultural Experiment Station, Fargo, pp 117–119.

Murray GM, Brennan JP (2009) Estimating disease losses to the Australian wheat industry. Australas Plant Pathol 38:558–570

Orolaza NP, Lamari L, Ballance GM (1995) Evidence of a host-specific chlorosis toxin from *Pyrenophora tritici-repentis*, the causal agent of tan spot of wheat. Phytopathology 85:1282–1287

Patel JS, Mamidi S, Bonman JM, Adhikari TB (2013) Identification of QTL in spring wheat associated with resistance to a novel isolate of *Pyrenophora tritici-repentis*. Crop Sci 53:842–852. https://doi.org/10.2135/cropsci2012.01.0036

Perez-Lara E, Semagn K, Tran VA, Ciechanowska I, Chen H, Iqbal M, N'Diaye A, Pozniak C, Strelkov SE, Hucl PJ, Graf RJ, Randhawa H, Spaner D (2017) Population structure and genome wide association analysis of resistance to disease and insensitivity to Ptr toxins in Canadian spring wheat using 90K SNP array. Crop Sci 57:1522. https://doi.org/10.2135/cropsci2016.10.0859

Poland JA, Brown PJ, Sorrells ME, Jannink JL (2012) Development of high-density genetic maps for barley and wheat using a novel two-enzyme genotyping-by-sequencing approach. PLoS ONE 7:e32253. https://doi.org/10.1371/journal.pone.0032253

See PT, Marathamuthu KA, Iagallo EM, Oliver RP, Moffat CS (2018) Evaluating the importance of the tan spot ToxA–*Tsn1* interaction in Australian wheat varieties. Plant Pathol 67(5):1066–1075. https://doi.org/10.1111/ppa.12835

Shabeer A, Bockus WW (1988) Tan spot effects on yield and yield components relative to growth stage in winter wheat. Plant Dis 72:599–602

Shankar M, Jorgensen D, Taylor J, Chalmers KJ, Fox R, Hollaway GJ, Neate SM, McLean MS, Vassos E, Golzar H, Loughman R, Mather DE (2017) Loci on chromosomes 1A and 2A affect resistance to tan (yellow) spot in wheat populations not segregating for tsn1. Theor Appl Genet 130:2637–2654. https://doi.org/10.1007/s00122-017-2981-6

Sharma JS, Zhang Q, Rouse MN, Klindworth DL, Friesen TL, Long Y, Olivera PD, Jin Y, McClean PE, Xu SS, Faris JD (2019) Mapping and characterization of two stem rust resistance genes derived from cultivated emmer wheat accession PI 193883. Theor Appl Genet 132:3177–3189. https://doi.org/10.1007/s00122-019-03417-x

Singh PK, Gonzalez-Hernandez JL, Mergoum M, Ali S, Adhikari TB, Kianian SF, Elias E, Hughes GR (2006) Identification and molecular mapping of a gene conferring resistance to *Pyrenophora tritici-repentis* race 3 in tetraploid wheat. Phytopathology 96:885–889

Singh PK, Mergoum M, Gonzalez-Hernandez JL, Ali S, Adhikari TB, Kianian SF, Elias EM, Hughes GR (2008) Genetics and molecular mapping of resistance to necrosis-inducing race 5 of *Pyrenophora tritici-repentis* in tetraploid wheat. Mol Breed 21:293–304

Singh PK, Singh RP, Duveiller E, Mergoum M, Adhikari TB, Elias EM (2010) Genetics of wheat–*Pyrenophora tritici-repentis* interactions. Euphytica 171:1–13. https://doi.org/10.1007/s10681-009-0074-6

Singh PK, Crossa J, Duveiller E, Singh RP, Djurle A (2016) Association mapping for resistance to tan spot induced by *Pyrenophora tritici-repentis* race 1 in CIMMYTs historical bread wheat set. Euphytica 207:515–525. https://doi.org/10.1007/s10681-015-1528-7

Somers DJ, Isaac P, Edwards K (2004) A high-density microsatellite consensus map for bread wheat (*Triticum aestivum* L.). Theor Appl Genet 109:1105–1114. https://doi.org/10.1007/s00122-004-1740-7

Soriano JM, Alvaro F (2019) Discovering consensus genomic regions in wheat for root-related traits by QTL meta-analysis. Sci Rep 9:1–14. https://doi.org/10.1038/s41598-019-47038-2

Soriano JM, Royo C (2015) Dissecting the genetic architecture of leaf rust resistance in wheat by QTL meta-analysis. Phytopathology 105:1585–1593. https://doi.org/10.1094/PHYTO-05-15-0130-R

Sosnowski O, Charcosset A, Joets J (2012) BioMercator V3: an upgrade of genetic map compilation and quantitative trait loci meta-analysis algorithms. Bioinformatics 28:2082–2083. https://doi.org/10.1093/bioinformatics/bts313

Stadlmeier M, Jørgensen LN, Corsi B, Cockram J, Hartl L, Mohler V (2019) Genetic dissection of resistance to the three fungal plant pathogens *Blumeria graminis*, *Zymoseptoria tritici*, and *Pyrenophora tritici-repentis* using a multiparental winter wheat population. G3 Genes Genomes Genet 9:1745–1757. https://doi.org/10.1534/g3.119.400068

Strelkov SE, Lamari L (2003) Host-parasite interactions in tan spot (*Pyrenophora tritici-repentis*) of wheat. Can J Plant Pathol 25:339–349

Sun X, Bockus W, Bai G (2010) Quantitative trait loci for resistance to *Pyrenophora tritici-repentis* race 1 in a Chinese wheat. Phytopathology 100:468–473. https://doi.org/10.1094/PHYTO-100-5-0468

Tadesse W, Hsam SLK, Zeller FJ (2006) Evaluation of common wheat cultivars for tan spot resistance and chromosomal location of a resistance gene in the cultivar 'Salamouni'. Plant Breed 125:318–322

Tadesse W, Hsam SLK, Wenzel G, Zeller FJ (2008) Chromosome location of a gene conferring resistance to *Pyrenophora tritici-repentis* in Ethiopian wheat cultivars. Euphytica 162:423–430

Taylor JD, Butler D (2015) ASMap: linkage map construction using the MSTmap algorithm. R Package Version 04-5

Van Ooijen JW (2006) JoinMap® 4, software for the calculation of genetic linkage maps in experimental populations. Kyazma BV, Wageningen, p 33

Venske E, dos Santos RS, da Rosa Farias D, Rother V, Maia LC, Pegoraro C, Costa De Oliveira A (2019) Meta-analysis of the QTLome of Fusarium head blight resistance in bread wheat: refining the current puzzle. Front Plant Sci 10:727. https://doi.org/10.3389/fpls.2019.00727

Virdi S, Liu Z, Overlander M, Zhang Z, Xu SS, Friesen T, Faris JD (2016) New insights into the roles of host gene-necrotrophic effector interactions in governing susceptibility of durum wheat to tan spot and *Septoria nodorum* blotch. G3 Genes Genomes Genet. https://doi.org/10.1534/g3.116.036525

Wang S, Wong D, Forrest K, Allen A, Chao S, Huang BE, Maccaferri M, Salvi S, Milner SG, Cattivelli L, Mastrangelo AM, Whan A, Stephen S, Barker G, Wieseke R, Plieske J, International Wheat Genome Sequencing Consortium, Lillemo M, Mather D, Appels R et al (2014) Characterization of polyploid wheat genomic diversity using a high-density 90 000 single nucleotide polymorphism array. Plant Biotechnol J 12:787–796. https://doi.org/10.1111/pbi.12183

Wu Y, Bhat PR, Close TJ, Lonardi S (2008) Efficient and accurate construction of genetic linkage maps from the minimum spanning tree of a graph. PLoS Genet 4:e1000212. https://doi.org/10.1371/journal.pgen.1000212

Yu L, Barbier H, Rouse MN, Singh S, Singh RP, Bhavani S, Huerta-Espino J, Sorrells ME (2014) A consensus map for Ug99 stem rust resistance loci in wheat. Theor Appl Genet 127:1561–1581. https://doi.org/10.1007/s00122-014-2326-7

Zhang Q, Faris JD, Chao S, Friesen TL, Zhong S, Cai X, Elias EM, Xu SS (2017) Identification and molecular mapping of quantitative trait loci for resistance to Fusarium head blight in cultivated emmer PI 272527 [abstract]. In: Proceedings of the 2017 National Fusarium head blight forum, December 3–5, 2017, Milwaukee, Wisconsin, p 97

Zhao X, Peng Y, Zhang J, Fang P, Wu B (2018) Identification of QTLs and meta-QTLs for seven agronomic traits in multiple maize populations under well-watered and water-stressed conditions. Crop Sci 58:507. https://doi.org/10.2135/cropsci2016.12.0991

Zou J, Semagn K, Chen H, Iqbal M, Asif M, N'Diaye A, Navabi A, Perez-Lara E, Pozniak C, Yang R-C, Graf RJ, Randhawa H, Spaner D (2017) Mapping of QTLs associated with resistance to common bunt, tan spot, leaf rust, and stripe rust in a spring wheat population. Mol Breed 37:144. https://doi.org/10.1007/s11032-017-0746-1